WADC TECHNICAL REPORT 52-89, PART 1

PLASTIC BEHAVIOR OF ENGINEERING MATERIALS

Part 1. Axial Tension and Bending Interaction Curves For Members Loaded Inelastically

D. O. BRUSH
O. M. SIDEBOTTOM
J. O. SMITH

UNIVERSITY OF ILLINOIS

AUGUST 1952

WRIGHT AIR DEVELOPMENT CENTER

NOTICES

When Government drawings, specifications, or other data are used for any purpose other than in connection with a definitely related Government procurement operation, the United States Government thereby incurs no responsibility nor any obligation whatsoever; and the fact that the Government may have formulated, furnished, or in any way supplied the said drawings, specifications, or other data, is not to be regarded by implication or otherwise as in any manner licensing the holder or any other person or corporation, or conveying any rights or permission to manufacture, use, or sell any patented invention that may in any way be related thereto.

The information furnished herewith is made available for study upon the understanding that the Government's proprietary interests in and relating thereto shall not be impaired. It is desired that the Judge Advocate (WCJ), Wright Air Development Center, Wright-Patterson Air Force Base, Ohio, be promptly notified of any apparent conflict between the Government's proprietary interests and those of others.

WADC TECHNICAL REPORT 52-89, PART 1

PLASTIC BEHAVIOR OF ENGINEERING MATERIALS

Part 1. Axial Tension and Bending Interaction Curves For Members Loaded Inelastically

D. O. Brush
O. M. Sidebottom
J. O. Smith

University of Illinois

August 1952

Materials Laboratory
Contract No. AF 33(038)-15677
RDO No. R-604-304

Wright Air Development Center
Air Research and Development Command
United States Air Force
Wright-Patterson Air Force Base, Ohio

McGregor & Werner, Inc., Wakefield, Mass.
Oct. 9, 1952 300

FOREWORD

This report was prepared by the Department of Theoretical and Applied Mechanics, Engineering Experiment Station, University of Illinois under Air Force Contract No. AF 33(038)-15677. The contract was initiated under the research and development project identified by Research and Development Order No. R-604-304, "Design Data for and Evaluation of Structural Metals"; it was administered under the direction of the Materials Laboratory, Research Division, Wright Air Development Center, with Dr. A. Herzog as project engineer.

ABSTRACT

This paper presents a theoretical method for constructing dimensionless interaction curves for members subjected to combined tension and bending loads that produce inelastic strains, and presents experimental results which verify the theory. Each interaction curve represents the total range of the ratios of axial load to bending moment which will cause inelastic strains to extend to a given depth in the member. Experimental interaction curves were obtained from eccentrically loaded tension members of rectangular cross sections made from three strain hardening materials, namely, annealed rail steel and aluminum alloys 24S-T4 and 75S-T6. Good agreement was found between theory and experiment. In order to design a member subjected to combined axial and bending loads by use of the interaction curves, the lateral deflection of the member must be estimated. Three orders of approximation for the lateral deflection of eccentrically loaded tension members are presented. The problem of combined bending and axial compressive loads is discussed and research based on the methods of analysis developed in this investigation is suggested for solving the buckling load of a member subjected to combined bending and axial compressive loads. Some illustrative problems are solved in the Appendix which show how the results of this investigation may be used.

PUBLICATION REVIEW

Manuscript Copy of this report has been reviewed and found satisfactory for publication.

FOR THE COMMANDING GENERAL:

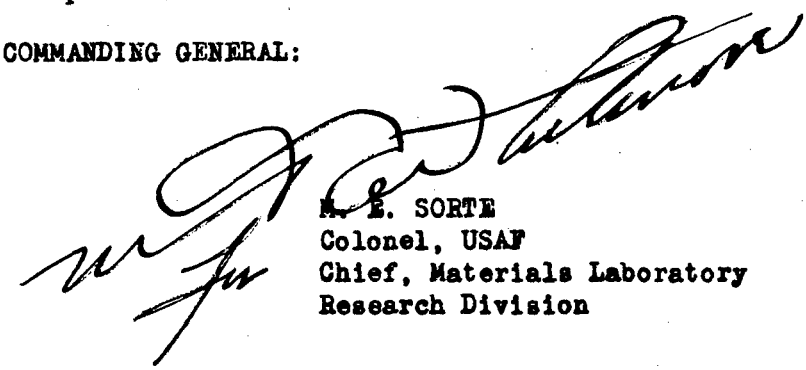

M. E. SORTE
Colonel, USAF
Chief, Materials Laboratory
Research Division

TABLE OF CONTENTS

LIST OF TABLES

LIST OF ILLUSTRATIONS

INTRODUCTION

Members of some machines and structures must be designed to resist loads where the weight of the members must be as low as possible. One way of obtaining such members is the use of light weight metals such as alloys of aluminum and magnesium. Another way has been by the improvement in the design of the cross-sections of the member by using sections made of thin sheets reinforced with stringers. Another important idea used in designing such a member is to take into account the increased resistance to loads by the member when relatively small inelastic strains are allowed to occur in the most strained fibers. This method requires the use of a relationship between the loads and the stresses or strains in the member when the strains exceed the elastic limit strain of the material. This method is important because it has been found that many members can resist loads that greatly exceed the maximum elastic load for the member. The maximum elastic load is the load at which the most strained fiber of the member is on the threshold of inelastic strain. For a member loaded in such a way that it has a stress gradient, the load necessary to produce a small amount of inelastic deformation of the most strained fibers may be appreciably larger than the maximum elastic load, especially if the stress gradient is steep at these fibers.

This investigation was undertaken to determine the influence of relatively small inelastic deformation on the loads carried by a member subjected to both an axial load P and a bending movement M. Small inelastic strains are here defined as those of the same order of magnitude as the elastic limit strain of the material. Some investigations have been made of such members, mostly of aircraft structural elements consisting of cross-sections made of thin sheets stiffened by stringers. There are many other types of

applications in which a member must be designed to carry combined bending and axial loads such as occurs when an eccentric load is applied to a tension member or to a compression member. For members loaded in compression, the failure of the member may be by elastic buckling if the member is relatively long, or by inelastic buckling if the member is relatively short. The behavior of a member that fails by inelastic buckling is complicated. Therefore, in this investigation the load P is a tensile load so that buckling failure does not occur. It was felt that the results of this investigation would give a better understanding of inelastic behavior of a member subjected to combined loads and lead to further research in the problem of inelastic buckling.

The failure of members tested in this investigation was by excessive inelastic deformation. None of the members was loaded to fracture, because of the fact that each member tested withstood inelastic strains over a major portion of its length and depth at the maximum loads used. It was, therefore, considered that each member failed by general yielding. As will be shown later, this general yielding was assumed to take place when inelastic strains had occurred at the most highly stressed cross-section to a certain arbitrarily chosen depth of the section.

When a member is subjected to a combination of two types of loads, such as P and M as used in this investigation, two relationships between the loads are necessary for the design of the member. The first relationship to be considered is that of the interaction curve which expresses the total range of values of load P and moment M which will result in a given depth of yielding. The second relationship expresses the relation between P and M for a given loading of a member so that a point on the interaction curve can be determined.

Method of Obtaining Interaction Curves

Inelastic strains impending. If no elastic strain can be allowed in a member similar to those shown in Fig. 6, the maximum stress σ in the extreme fibers can be written in terms of P and M by using the principle of superposition. This expression is

$$\sigma = \frac{P}{A} + \frac{Mc}{I}$$

in which A is the cross-section area, c is the distance from the centroid to the extreme fiber, and I is the moment of inertia of the area with respect to the centroidal axis. If the value of σ is equal to the elastic limit σ_e of the material the foregoing equation states the condition that inelastic strain is impending or is on the verge of occurring in the most stressed fibers. The equation is transformed by dividing both sides by σ_e and setting $P_e = \sigma_e A$ and $M_e = \sigma_e I/c$ where P_e and M_e are the elastic limit loads for the member for axial tension only and pure bending only, respectively,

$$\frac{P}{P_e} + \frac{M}{M_e} = 1 \qquad (1)$$

Equation (1) is represented by the line DC in Fig. 4 in which ordinates represent values of M/M_e and abscissas P/P_e. The curve DC (straight line in this case) represents corresponding pairs of values of M and P which will cause the member to be on the verge of starting to strain inelastically and is called an interaction curve. Equation (1) constitutes a relationship between P and M for impending inelastic strains, but an additional relationship between P and M must be found for a given member subjected to a combination of bending and axial loads. For the case considered here, namely, eccentric tensile loads, this additional equation is

$$M = P(e_o - \Delta) \qquad (2)$$

in which e_o (See Fig. 6) is the initial eccentricity and Δ is the deflection of the member at its middle section. For impending inelastic strains Δ is equal to Δ_e. In order to determine the pair of values of P and M that correspond to impending inelastic strain, we must determine[+] Δ_e and then solve Eq. (1) and (2) simultaneously. If e_o is relatively large, the effect of Δ_e is usually neglected, that is, Eq. (2) is written $M = Pe_o$. An indefinitely large value of e_o corresponds to the case of pure bending.

Small Inelastic Strain Allowed. The loads M and P, as given by the foregoing equations, will have to be increased somewhat in order to cause inelastic strains to occur at the extreme fiber and at other nearby fibers in the most highly stressed cross-section. Eventually, if the loads M and P are increased sufficiently, the fibers at all depths in the beam at the most highly stressed cross-section will become inelastically strained; however, this condition will result in an inelastic deformation which can no longer be considered small and the member will have failed by general yielding. Therefore, some compromise loading between the loads which result in failure by general yielding and the loads that cause inelastic strains to be impending in the extreme fiber is desirable. In this paper the loads chosen are those combinations of M and P that cause inelastic strains to occur over one-half the depth of the most highly stressed cross-section. This choice of proportions of area covered by elastically strained as compared with inelastically deformed fibers is made because it leaves half of the section elastic which insures that the deformation of the member is of the same order of magnitude as that which occurs under the elastic limit loads when inelastic strains are impending. Furthermore, this manner of describing the extent

---

[+]See Appendix to this paper. Also see Airplane Structures, A. S. Niles and J. S. Newell, John Wiley and Sons, Vol. II, 3rd Ed., 1943, p. 67.

and magnitude of inelastic strains is more convenient to use than methods which make use of magnitude of the maximum stress or strain. Also it more closely describes the approach condition of the member to failure by general yielding.

The interaction curve for the condition described in the preceding paragraph, namely, the loads corresponding to inelastic strains in one-half the depth of the most highly stressed section cannot be found by use of the principle of superposition as was Eq. (1), and is found here by plotting a few points. The method used is to assume that at this cross-section an arbitrary distribution of the strains is chosen which makes half the depth inelastic and half elastic as previously described. The problem is to determine what load P and bending moment M corresponds to the assumed strain distribution (see Fig. 2b and c). An example is now given which shows how the interaction curve is drawn. ABC in Fig. 1 represents the interaction curve for inelastic strain to one-half depth of the cross-section of a member of rectangular cross-section made of a material having equal yield points σ_e in tension and compression, that is, the slope α (Fig. 2) of the stress strain curve is zero when the stress becomes σ_e. The ordinate of point A which corresponds to pure bending is obtained by finding the moment $M = \int \sigma y dA$. In this integral y is measured from the centroid and the distribution of the stress σ on the beam cross-section is as shown by the figure near the point A. In this case inelastic strains are assumed to occur at the top and bottom of the beam to one-fourth its depth, that is, a total of one-half. The moment M is divided by $M_e = \sigma_e I/c = \frac{2}{3} \sigma_e bc^2$. The abscissa of A is zero since $P = \int \sigma dA$ is zero for this stress distribution. Similarly, the ordinate of B is found by determining M from the integral $M = \int \sigma y dA$ in which the stress distribution is shown in the figure near B and y is again measured from the centroidal axis. In this case all inelastic strains are

assumed to occur in the upper one-half of the cross-section and inelastic strains in lower extreme fiber are impending. This value of M is equal to $\frac{2}{3}\sigma_e bc^2$ for the rectangular section and, since $M_e = \frac{2}{3}\sigma_e bc^2$, the ratio $M/M_e = 1$ is the ordinate of B. The abscissa of B is found by determing the resultant force $P = \int \sigma dA$ for the stress distribution on the section. This value is $P = \sigma_e bc$ for the rectangular section and therefore $P/P_e = 1/2$. It is proved later that from B to C the curve is always a straight line. Because of this fact the location of the point B is very important. Other points between A and B can be found in a manner similar to that used in locating A and B. When α is not zero (see Fig. 2a) the interaction curve can be drawn in exactly the same way that ABC was drawn. In Fig. 1 the curves A'''B'''C, A"B"C and A'B'C' represent the interaction curve for materials in which $\alpha = \alpha_1 = \alpha_2$ is 0.2, 0.6 and 1.0, respectively. It will be shown later that curves for values of α between 0 and 1, such as A'''B'''C and A"B"C, can be drawn by linear interpolation between ABC($\alpha = 0$) and A'B'C($\alpha = 1$).

An interaction curve such as ABC in Fig. 1 represents one relationship between P and M. Equation (2), called the moment-load relationship in this paper, is an additional relationship which can be used to solve for the desired values of P and M for a given problem. But in order to use Eq. (2), the value of $\triangle$ must be known. A value of the deflection $\triangle$ can be determined approximately by making use of the assumed depth of inelastic strain in the member. Simple procedures are presented later to give first, second, and third approximations to the deflection of a member loaded eccentrically in tension. The shape of an interaction curve in the inelastic range is a function of the cross-section[+] of the member (Fig. 5), the shape of the

[+]For a discussion of interaction curves for various types of cross-sections see F. B. Seely and James O. Smith, "Advanced Mechanics of Materials," Second Edition, John Wiley and Sons, 1952.

stress-strain diagram of the material (Fig. 1), and the depth of yielding (Fig. 4).

Several assumptions have been made in constructing these interaction curves. The tension and compression stress-strain diagrams are assumed to be represented by two straight lines as indicated in Fig. 2a. Plane sections are assumed to remain plane. It is further assumed that a plane given by the action line of the load and the centroidal axis of the member is a plane of symmetry of the cross-section.

Proof that BC is straight line. The proof of the linearity of line BC and the location of point B will now be given for a beam of rather general cross sections such as that shown in Fig. 2c and for a general case. The beam is subjected to a load P and moment M such that the depth of yielding is a and the maximum compressive stress σ_2 is less than σ_{e_2} (see Fig. 2a and 2b). The equations of equilibrium for the stress distribution are

$$P = \int \sigma dA \; ; \quad M = \int \sigma y dA \tag{3}$$

where y is measured from the centroidal axis. The stresses in the elastic and inelastic region are, respectively

$$\sigma = \frac{\sigma_{e1} - \sigma_2}{h - a} (c_2 + y) + \sigma_2$$

$$\sigma = (1 - \alpha)\, \sigma_{e1} + \frac{\alpha(\sigma_{e1} - \sigma_2)}{h - a} (c_2 + y) + \alpha\sigma_2$$

in which σ_2 is negative for compression. If these stresses are put in Eq. (3), the load and moment in dimensionless form are

$$\frac{P}{P_e} = \frac{1 - \beta}{A(h-a)} (c_2 A_e + Q_e + \alpha c_2 A_p + \alpha Q_p) + \beta \frac{A_e}{A} + \alpha\beta \frac{A_p}{A} + (1-\alpha) \frac{A_p}{A} \tag{4}$$

$$\frac{M}{M_e} = \frac{1-\beta}{h-a}\frac{c_1}{I}(c_2Q_e + I_e + \alpha c_2Q_p + \alpha I_p) + \frac{\beta c_1 Q_e}{I} + \frac{\alpha\beta c_1 Q_p}{I} + (1-\alpha)\frac{c_1 Q_p}{I} \qquad (5)$$

where $P_e = \sigma_{e1}A$, $M_e = \frac{\sigma_{e1}I}{c_1}$, $\beta = \frac{\sigma_2}{\sigma_{e1}}$ (negative for σ_2 compression), and Q is first moment of the area about centroidal axis. The subscripts e and p on A, Q, and I refer to the elastic and inelastic (plastic) areas of the cross-section.

For a given cross-section, a given depth of inelastic deformation, and a given material, all the terms on the right side of either Eq. (4) or (5) are constant except β. Since P and M are both linear in β, the line BC is a straight line. If σ_2 is made equal to $-\sigma_{e2}$, the yield stress in compression, Eq. (4) and (5) can be used to locate the point on the interaction curve corresponding to point B in Fig. 1.

For the special case of a rectangular cross-section with $A = \frac{h}{2}$, $\sigma_{e2} = \sigma_{e1}$ and $\beta = -1$, Eq. (4) and (5) become

$$\frac{P}{P_e} = \frac{1}{2} + \frac{a}{2}$$

$$\frac{M}{M_e} = 1 + a \qquad (6)$$

If a is set equal to zero in Eq. (6), point B in Fig. 1 is obtained. Point B' is obtained if a is equal to unity. The load P and the moment M vary linearly with a so that the point corresponding to point B for a material with $a = 0$ must lie on the straight line BB'. It should be observed that the general expression for P and M, Eq. (4) and (5), are also linear in a. The point on the interaction curve corresponding to B in Fig. 1 for any value of a is obtained by interpolation between B and B', that is, by laying off a distance along BB' from B equal to aBB'.

For any point on the interaction curve from A to B inelastic strains

occur on both sides of the member. In the more general case the location of any point on this curve is a function of both α_1 and α_2, the strain hardening factors in tension and compression. If $\alpha_1 = \alpha_2 = \alpha$, the location of any point from A to B can be computed for $\alpha = 0$ and $\alpha = 1$ and the location of the point for any α can be determined by interpolation in a manner similar to that discussed above for point B. The curves shown in Fig. 1 illustrate the effect of α on the interaction curves for 1/2 depth of yielding in a member with rectangular cross-section.

The calculation of a point on the interaction curve for the more general case can be carried out from diagrams similar to that shown in Fig. 3. Assume a strain distribution, Fig. 3a, which will result in a given depth of yielding. From the strain distributions and the known stress-strain diagrams, Fig. 2a, the stress distribution, Fig. 3b, can be obtained. The load P and the moment M can then be calculated for the given stress distribution.

The effect of depth of yielding on the interaction curves is shown in Fig. 4 for a member with rectangular cross-section and made of a material with identical properties in tension and compression and $\alpha = 0$. The effect of cross-section on the interaction curves is indicated in Fig. 5 by the rectangular, circular, and T-cross-sections. The material is the same as for the curves shown in Fig. 4, and the depth of yielding is 1/2 the depth of the member.

For a member of given length, cross-section, and initial eccentricity, the load or moment on the member necessary to produce a given depth of yielding cannot be determined unless the deflection of the member for these conditions is known. If the deflection is known, the final eccentricity can be calculated and the relation between moment and load obtained. In case the axial eccentric load is a tension load, simple first, second, and third

approximations to the moment-load curves are given later in this paper so that a safe approximation to the load can be obtained. These procedures are presented in the discussion of results.

Materials and Method of Testing

The materials used in the experimental investigations were annealed high carbon rail steel and aluminum alloys 24S-T4 and 75S-T6. Nine eccentrically loaded tension members were tested, three for each material. The rail steel test members were machined from the base of an annealed railroad rail. The aluminum test members were machined from six pieces of as-rolled bar stock. All machined surfaces were finish ground. The overall dimensions of the test members are shown in Fig. 6. The numerical values of the cross-sectional dimensions and the original eccentricity, e_o, are listed in Table 1.

The test members were all tested in a hydraulic type, Amsler testing machine having load ranges of 0 to 10,000, 0 to 20,000, 0 to 50,000, and 0 to 100,000 lb. The load was applied by the fixtures shown in Fig. 7. The two yokes were attached to the heads of the testing machine. The load was transmitted from the yoke through 3/8 in. diameter hardened steel balls to the tapered pin and from the pin to the test member. The purpose of the taper on the pin was to permit lateral adjustment of the test member to minimize lateral bending.

Strains in the rail steel members were measured by one inch, Type A-11, SR-4, electrical strain gages at the locations shown in Fig. 6. These gages were not found to be reliable for the large tensile strains (up to 0.015 in. per in.) in the aluminum members; therefore, a two inch gage length mechanical extensometer, with one division on the dial equaling 0.0001 in. per in. strain, was used to measure the strains in the fibers near the most strained fibers. The data from the SR-4 gage was used for small strains and the

Table I. Original Eccentricities and

Original Cross-Sectional Dimensions of Test Members

Material	Test Number	b Breadth of Section in.	d Depth of Section in.	e_o Original Eccentricity in.
Annealed Rail Steel	1	0.753	1.249	1.147
	2	0.753	1.249	0.465
	3	0.753	1.249	0.282
Aluminum Alloy 24S-T4	1	0.751	1.252	1.194
	2	0.751	1.252	0.503
	3	0.751	1.252	0.304
Aluminum Alloy 75S-T6	1	0.747	1.252	1.194
	2	0.747	1.252	0.504
	3	0.501	1.252	0.304

extensometer was used for large strains. The deflections of the members were measured by a 1/10000 in. dial by the arrangement shown in Fig. 7.

In testing, increments of load were applied and corresponding strains and deflections measured. In the inelastic range the strain and deflection readings indicated that the inelastic deformation continued with time. In such cases an arbitrary time interval of 5 to 15 minutes was allowed for indicators to become reasonably steady before readings were taken. During this interval a fairly successful attempt was made to hold the load at a constant value.

Properties of Materials

Mechanical properties of the materials were determined from standard tension and compression specimens cut from the bars from which the moment-load test members were made. They were selected so that the center lines of the tension and compression specimens coincided as nearly as possible with the most strained tension and compression fibers of the moment-load test members. Three tensile specimens were tested for the annealed rail steel, one near most strained fibers of each of the three test members. From past experience with this material, it was assumed to have the same properties in tension and compression. For each aluminum alloy, three tension and two compression specimens were tested. The stress-strain diagrams of the materials are shown in Fig. 8 and 9. Each diagram is shown approximated by two straight lines. Mechanical properties were taken from these straight lines and are listed in Table II.

Discussion of Results

For each of the nine eccentrically loaded tension members, the strain distributions across the depth of the member and the deflections were obtained at increasing loads. The strains were measured at the locations shown

Table II. Mechanical Properties of Materials

Material	E 10^6 psi.	Tension		Compression	
		σ_{e1} psi.	a_1	σ_{e2} psi.	a_2
Rail Steel					
Test Member No. 1	30.9	38,600	0.082		
Test Member No. 2	30.9	37,000	0.077		
Test Member No. 3	30.9	36,000	0.077		
24S-T4	10.9	49,600	0.035	40,800	0.123
75S-T6	10.4	72,000	0.024	70,800	0.100

in Fig. 6. In the case of the six aluminum specimens, the strains in the most stressed tension fibers for elastic conditions were measured by the SR-4 gages. Thereafter these strains were obtained by extrapolation using the strains as determined by the 2 inch extensometer.

The load P on each member was weighed by the testing machine. The moment M corresponding to P was calculated from the load P, the initial eccentricity e_o and the measured deflection. Each load P and moment M was reduced to dimensionless form by dividing by the respective quantities $P_e = \sigma_{e1} A$ and $M_e = \frac{\sigma_{e1} I}{c}$ where σ_{e1} is the yield stress in tension as listed in Table II. Corresponding values of the dimensionless ratios of load and moment are plotted for each of the test specimens in Fig. 10, 11 and 12 for the annealed rail steel, aluminum alloy 24S-T4, and aluminum alloy 75S-T6, respectively. In each of these figures are shown theoretical interaction curves for the loads P and M which, when acting together, will cause inelastic strains of fibers to zero depth, one-quarter depth, and one-half depth, respectively, across the section of the member. For each of the test members a test point was determined for each of the interaction curves and each is shown as a circle with a dot in the center. The test points indicate that the largest error in the calculation of either the moment or load was less than 5 %.

Approximate Methods of Determining the Deflection Δ in Eq. (2). In the following paragraphs three approximations of the moment-load curves will be presented for obtaining conservative values of the load necessary to produce a given depth of inelastic strain. In each case the actual deflection is larger than that computed, but the use of an interaction curve such as ABC in Fig. 1 with Eq. (2), in which either of the values of Δ is substituted, for computing P for a member such as in Fig. 6 will give a

conservative value of P, that is, the value of P will be less than that which will be required to cause the actual assumed conditions in the member. This fact will be discussed under the next sideheading.

For the first approximation of the moment-load curve, (Eq. (2)) assume that the member does not deflect so that the relation between load and moment can be calculated from the initial eccentricity. The radial solid lines shown in Fig. 10, 11, and 12 represent the first approximation to the moment-load curves.

For the second approximation of the moment-load curve, we calculate the maximum elastic deflection Δ_e (See Appendix) corresponding to a stress of σ_{e1} or σ_{e2} in the extreme fiber, depending on whether yielding begins on the tension or compression side. The relation between load and moment based on the eccentricity corrected for elastic deflection are shown as dashed lines in Fig. 10, 11 and 12.

A third approximation of the moment-load curves is easily obtained for any given depth of yielding. For the special case of pure bending of a beam whose cross-section has two planes of symmetry and made of a material with identical stress-strain diagrams in tension and compression, the deflection of the beam is obtained in terms of the maximum elastic deflection Δ_e. From geometrical considerations it can easily be shown that, for these conditions,

$$\frac{\Delta}{\Delta_e} = \frac{1}{1 - \psi} \qquad (7)$$

where Δ_e is the maximum elastic deflection corresponding to an extreme tensile fiber stress of σ_{e1} and ψ is the total depth of yielding, including yielding on both sides when it occurs, divided by the depth of the beam. For ψ equal to 1/4 or 1/2 Eq. (7) gives deflection of $\frac{4}{3}\Delta_e$ and $2\Delta_e$, respectively.

The computation by the more exact method of the deflection after inelastic strains have occurred requires an enormous amount of work. The third approximation of the moment-load curves is also based on a deflection which is smaller than the actual deflection. This is explained as follows. It is assumed that the lateral deflection of the member is proportional to the algebraic difference of the strains in the most strained tension and compression fibers of the member. Consider as a special case an eccentrically loaded member in which the strain in the most strained compression fibers does not change as inelastic deformation occurs; the deflection of this member is given by Eq. (7). This special case does not occur except perhaps for small eccentricities accompanied by large depth of yielding, and hence the strain on the compression side increases as yielding takes place so that the algebraic difference in strain is larger than that necessary for Eq. (7) to be valid. Hence, in general, the actual lateral deflection will be larger than that given by Eq. (7). The dotted lines in Fig. 10, 11 and 12 were obtained by using Eq. (7), in which ψ was made equal to 1/2.

Error due to use of Approximate Δ. The load P obtained by using these lines which represent the first, second, and third approximation are all smaller than the actual value of P and the value of M is larger than its actual value as shown by the larger circle with black dot in Fig. 10, 11 and 12.

It is sometimes desirable to use in Eq. (2) an approximate value of Δ which is slightly larger than the actual value. This procedure would lead to the computation of values of P and M that are, respectively, slightly larger and slightly smaller than the values that will cause the actual inelastic strained condition of the member that is assumed. The following method is used for determining such a value of Δ.

From the calculations for the maximum elastic load, the neutral axis

and the strains ε_e, and $-\varepsilon_2$ for the most strained tension and compression fibers can be determined; the strains will be ε_1 and $-\varepsilon_{e2}$ if impending yielding is on the compression side. By assuming that the neutral axis does not shift, the strains ε_1 and $-\varepsilon_2$ in the most strained fibers can be determined for a given depth of yielding. If the deflection is assumed to be proportional to the algebraic difference of the strains, the deflection can be computed by the expression

$$\Delta = \frac{\varepsilon_1 - (-\varepsilon_2)}{\varepsilon_{1e} - (-\varepsilon_2)} \Delta_e \qquad (8)$$

for the case in which yielding initiates on the tension side. This value for the deflection will be larger than the actual deflection since the neutral axis shifts toward the compression side of the member thus reducing both ε_1 and ε_2 for a given depth of yielding.

Axial Compression and Bending Loads. The results of the investigation reported here do not usually apply to a member subjected to combined bending and axial loads if the axial load is a compressive load. The reason for this fact is described as follows. When the axial load is a tensile load its effect is to reduce the deflection due to bending and it thereby tends to reduce the maximum bending moment. This is shown by the fact that in Fig. 10, 11 and 12, where the axial load is a tensile load, the test data representing values of maximum bending moment M versus the axial load P lie in curves which are concave downward and to the right. On the other hand, when the axial load is a compressive load its effect is to increase the deflection due to bending and it thereby tends to increase the maximum bending moment. This is shown in Fig. 13 where some assumed moment-load curves OBD and OFG resulting from compressive axial loads are shown (no tests were made using compressive axial loads; this important problem requires further

research). In Fig. 13 curve OAC represents an actual test of a member of 75S-T6 under combined bending and axial tensile loads and this curve shows that the tensile axial load reduces the deflection so much that the bending moment reaches a maximum as shown at A. On the other hand, the hypothetical[+] curve OBD for the same member subjected to combined bending and axial compressive loads is concave upward and to the left, showing that the compressive axial load tends to increase the bending moment. Curve OBD shows, by the vertical tangent at B, that, when the axial load is compressive, the axial load reaches a maximum value, instead of the bending moment. This fact means that when the axial compressive load represented by the abscissa of the point B is applied to this member it becomes unstable and will collapse by buckling, because points on the curve above B show that, when the load at B is reached, smaller axial compressive loads than at B are capable of producing greater bending moments.

It should be noted that the curve OBD does not intersect the curve representing pairs of values of M and P that correspond to 1/2 depth of the section being inelastically strained, and hence the results of the analysis in this report do not apply to such members. However, if the member is subjected to a compressive axial load having only a small eccentricity, the moment-load curve may be represented by a curve such as OFG which does intersect the curve representing 1/2 depth of inelastic strain before the buckling load at F is reached. It is of interest here to note that the points B and F will always be above the line representing the beginning of yielding. This means that the primary buckling (collapse) load for a member subjected to combined bending and axial compressive loads corresponds to a combination of bending moment and axial loads that will produce some inelastic strain in the most highly stressed cross-section.

[+] A procedure for constructing the moment-load curves for members loaded in compression has been developed by W. D. Jordan but has not as yet been published.

Additional research is needed for solving the problem of combined bending and axial compressive loads. It is believed that the method of attack used in this investigation can be used for this purpose.

Summary and Conclusions

A method is presented for constructing dimensionless interaction curves for any members of any cross-section having one axis of symmetry and subjected to eccentric axial loads in the plane of symmetry. The theoretical interaction curves for members of rectangular cross-section were compared with experimental data for eccentrically loaded tension members of annealed rail steel and aluminum alloys 24S-T4 and 75S-T6. Three specimens of each material were tested to give three points on each interaction curve. Four approximations to the lateral deflection of a member are presented so that a satisfactory approximation of the loads for a given depth of yielding can be computed. The results presented in this paper are believed to be sufficient to justify the following conclusions:

1. The interaction curve is constructed for a given member subjected to a combination of axial load and bending moment by locating two or more points on the curve. Each point is located by computing the values of P and M for the stress distribution that is assumed to occur for the given depth of inelastic strain. Because of the ease of construction and use, the interaction curve was derived to give the range of corresponding values of moment and load which would produce a given depth of inelastic strain. The tension and compression stress-strain curves for the material are approximated by two straight lines (see Fig. 8 and 9).

2. The results obtained from tests of eccentrically loaded rectangular tension members of annealed rail steel and aluminum alloys 24S-T4 and 75S-T6 gave good correlation between theoretical and experimental interaction

curves.

3. In designing an eccentrically loaded tension member for a given depth of yielding, the lateral deflection in Eq. (2) for the member must be known so that the relation between axial load and bending moment can be determined. Four approximations to the moment-load curve are presented. All approximations give values of P and M that are not greatly different from the values which correspond to the actual conditions assumed in the member.

4. In the Appendix to this report, illustrative examples show that for beams of rectangular cross-section subjected to combined axial tension and bending loads more than 50 percent increase in load at the threshold of the occurrence of inelastic strain in the most highly stressed fibers of the beam is required to cause inelastic strains in the most stressed cross-section to occur to a depth of 1/2 the cross-section.

5. The results of this investigation are not generally applicable to such members as described in the foregoing conclusions when the axial load is a compressive force. This problem is one of unstable equilibrium because the axial load reaches a maximum and at this load the member will collapse due to inelastic buckling. It is concluded that further research, in which moment-load curves, such as OBD and OFG in Fig. 13, must be used, will be required to solve this problem. The method of analysis developed in this report will be of great value in analyzing the behavior of a member subjected to combined bending and axial compressive load.

ACKNOWLEDGMENTS

The investigation was carried out as part of the work of the Engineering Experiment Station of the University of Illinois, of which Dean W. L. Everitt is the Director, in the Department of Theoretical and Applied Mechanics, of which Professor F. B. Seely is the Head. It was part of an investigation sponsored by the Wright Air Development Center, Wright-Patterson Air Force Base, Ohio. Acknowledgment is made to Mr. Che-Tyan Chang for his help in the analysis.

APPENDIX I

ILLUSTRATIONS SHOWING USE OF INTERACTION CURVES

Introduction--In making use of Eq. 2 as one of the relationships between the combined loads M and P the deflection Δ is sometimes neglected, that is, Δ is set equal to zero. When more accurate results are desired a value of Δ is given in terms of the maximum deflection Δ_e and ψ by Eq. 7, where Δ_e is the deflection of the member when the most strained fiber at the most highly stressed cross-section is on the threshold of becoming inelastically strained, and ψ represents the ratio of the total depth of the inelastic strain at this section to the total depth of the cross-section. The following example illustrates the method of computing the values of the deflection and bending moment in a member subjected to combined axial and bending loads and of making use of the interaction curves in this report to solve for the loads on such a member that correspond to a given depth of inelastic strain in the most highly strained cross section of the member.

Computation of Maximum Deflection and Maximum Moment--Fig. 14 represents a beam of length ℓ, simply supported at its ends, that is subjected to the following loads: a concentrated load W at its mid-point, bending moments M_1 at its ends and an axial load P. The deflection of the beam at the distance x from the left end is y. The bending moment at any section in the left one-half of the beam is

$$M = M_1 + Py - \frac{Wx}{2} \qquad (9)$$

If the value of M from Eq. 9 is substituted in the equation $EI \frac{d^2y}{dx^2} = M$ it becomes

$$\frac{d^2y}{dx^2} - \frac{P}{EI}y = \frac{M_1}{EI} - \frac{W}{2EI}x \qquad (10)$$

The solution of Eq. 10 is

$$y = C_1 \sinh \sqrt{\frac{P}{EI}}\, x + C_2 \cosh \sqrt{\frac{P}{EI}}\, x - \frac{M_1}{P} + \frac{W}{2P}\, x \qquad (11)$$

The constants C_1 and C_2 are determined from the fact that $y = 0$ when $x = 0$ and that $\frac{dy}{dx} = 0$ when $x = \frac{\ell}{2}$. When these values of C_1 and C_2 are found and x is set equal to $\frac{\ell}{2}$ the maximum deflection is found to be

$$\Delta_{max} = \frac{1}{P}\left[-\frac{W}{2}\sqrt{\frac{EI}{P}} \tanh \frac{\ell}{2}\sqrt{\frac{P}{EI}} + M_1\left(\frac{1}{\cosh \frac{\ell}{2}\sqrt{\frac{P}{EI}}} - 1\right) + \frac{W\ell}{4}\right] \qquad (12)$$

Furthermore if Eq. (11) is differentiated twice with respect to x and if both sides are then multiplied by EI the resulting expression represents the bending moment at any section. The maximum bending moment usually occurs at $x = \frac{\ell}{2}$, depending upon the relative values of the loads, and is found from the above to be

$$M_{max} = -\frac{W}{2}\sqrt{\frac{EI}{P}} \tanh \frac{\ell}{2}\sqrt{\frac{P}{EI}} + \frac{M_1}{\cosh \frac{\ell}{2}\sqrt{\frac{P}{EI}}} \qquad (13)$$

Equation (10), (11), (12), and (13) are valid only so long as the most strained fibers in the beam are elastically strained.

ILLUSTRATIVE PROBLEMS

Problem 1. Let the beam in Fig. 14 be made of aluminum alloy 75S-T6 (see Table II for properties) and have a rectangular cross-section whose depth is $2c = 1.25$ in. and width is $b = 0.75$ in. The length is $\ell = 8.25$ in. Let the load $W = 0$ and the moment $M_1 = Pe_o$. This beam is that of Fig. 6. Let $e_o = 0.3$ in. (a) Compute the value of the load P that will cause the most highly stressed fiber in the most highly stressed cross-section (section of maximum bending moment) in the beam to be on the threshold of inelastic strain and compute the maximum deflection Δ_e for this load. (b) Compute the value of the load P that will cause inelastic strains to occur over one-half the depth

of the most highly stressed cross-section, that is, the section where the maximum bending moment occurs.

Solution: (a) Load for Inelastic Strain Impending. When W is set equal to zero and $M_1 = 0.3P$, Eq. (13) is

$$M = \frac{0.3P}{\cosh \frac{\ell}{2}\sqrt{\frac{P}{EI}}} \tag{14}$$

We must now solve Eq. (1) and (14) simultaneously for values of M and P. It is more convenient to do this if Eq. (14) is divided by M_e so that it contains the dimensionless ratios $\frac{M}{M_e}$ and $\frac{P}{P_e}$. This transformation of Eq. (14) results in the following equation

$$\frac{M}{M_e} = \frac{0.9\,\frac{P}{P_e}}{c\cosh \frac{\ell}{2}\sqrt{\frac{3\sigma_e}{Ec^2}\,\frac{P}{P_e}}} \tag{14a}$$

The following equation results when Eq. (1) is subtracted from Eq. (14a).

$$-\frac{P}{P_e} = \frac{0.9\,\frac{P}{P_e}}{c\cosh \frac{\ell}{2}\sqrt{\frac{3\sigma_e}{Ec^2}\,\frac{P}{P_e}}} - 1 \tag{15}$$

The values $c = 0.625$, $E = 10{,}900{,}000$ lb/in^2 and $\sigma_e = 72000$ lb/in^2 are substituted in Eq. (15) which is solved by trial and error for $\frac{P}{P_e}$. The result is that $\frac{P}{P_e} = 0.45$ and $\frac{M}{M_e} = 0.55$ and since $P_e = 2bc\sigma_e = 2 \times 0.75 \times 0.625 \times 72000 = 67500$ lb, the load is $P = 30400$ lb. These computed values represent the actual values found in the test. The deflection Δ_e is obtained from Eq. (12) by the substitution of this value of P with the other quantities given in this problem. The result is

$$\Delta_e = \frac{1}{30400}\left[0.3 \times 30400\left(\frac{1}{\cosh 0.62} - 1\right)\right] = 0.05 \text{ in.}$$

(b) Load for Inelastic Strain to One-Half Depth. For this solution we use Eq. (2) and the interaction curve marked 1/2 depth in Fig. 12. Equation (2) is

$$M = P(e_o - \Delta) \qquad (2)$$

The value of Δ to be used in Eq. (2) is obtained from Eq. (7) and is

$$\Delta = \frac{\Delta_e}{1 - \psi} \qquad (7)$$

and by making $\Delta_e = 0.05$ in. and $\psi = 1/2$, we find

$$\Delta = 0.10 \text{ in.}$$

Therefore, from Eq. (2)

$$M = P(0.3 - 0.10) = 0.20P$$

We transform this latter equation into dimensionless ratios by dividing both sides by M_e so that

$$\frac{M}{M_e} = \frac{0.2P}{M_e} = \frac{0.2P}{\frac{\sigma_e I}{c}} = \frac{0.6}{c}\frac{P}{P_e} = 0.96\frac{P}{P_e}$$

This equation is represented by the dotted line OB in Fig. 12. The coordinates of the point B, which are

$$\frac{M}{M_e} = 0.66 \text{ and } \frac{P}{P_e} = 0.69,$$

represent the desired values of P and M. Therefore

$$P = 0.69\ P_e = 0.69 \times 67500 = 46{,}500 \text{ lb.}$$

The coordinates of the black centered circle at C represent the actual values determined from the test which were $\frac{M}{M_e} = 0.60$ and $\frac{P}{P_e} = 0.71$, that is, the test value of P = 48,000 lb.

A comparison of the 46,500 lb. with 30,400 lb. shows that a 53 % increase in the load at the threshold of occurrence of inelastic strain is required to cause inelastic strains in the most stressed cross-section to occur

to a depth of 1/2 the cross-section. The actual value of this load as found by tests was 58 °/o higher.

Problem 2. Solve Problem 1 with the load W = - P, instead of W = 0. The negative sign means that W acts downward and the reactions $\frac{W}{2}$ downward, that is, in the reverse sense from that in Fig. 14. All other loads are the same and the dimensions and material are the same as in Prob. 1.

Solution. (a) Load for Inelastic Strain Impending. In Eq. (14) we set W = - P and $M_1 = Pe_o$. We then transform the equation by dividing both sides by M_e to get $\frac{M}{M_e}$ on the left side and by adjusting the quantities on the right side and under the radicals, etc., so that the term $\frac{P}{P_e}$ appears where P occurs. When this is done, Eq. 13 becomes

$$\frac{M}{M_e} = \frac{3e_o}{c} \frac{\frac{P}{P_e}}{\cosh\left(\sqrt{\frac{3}{4}\frac{\ell^2}{c^2}\frac{\sigma_e}{E}\frac{P}{P_e}}\right)} + \sqrt{\frac{3}{4}\frac{E}{\sigma_e}\frac{P}{P_e}} \tanh\left(\sqrt{\frac{3}{4}\frac{\ell^2}{c^2}\frac{\sigma_e}{E}\frac{P}{P_e}}\right) \qquad (15)$$

Eq. 1 is subtracted from the Eq. 15 with the following result

$$1 = \frac{P}{P_e}\left[1 + \frac{3e_o}{c} \frac{1}{\cosh\left(\sqrt{\frac{3}{4}\frac{\ell^2}{c^2}\frac{\sigma_e}{E}\frac{P}{P_e}}\right)}\right] + \sqrt{\frac{3}{4}\frac{E}{\sigma_e}\frac{P}{P_e}} \tanh\left(\sqrt{\frac{3}{4}\frac{\ell^2}{c^2}\frac{\sigma_e}{E}\frac{P}{P_e}}\right)$$

The values of e_o, c, ℓ, σ_e and E are substituted in this equation from this problem and the equation is solved by trial and error for the value of $\frac{P}{P_e}$ which is found to be $\frac{P}{P_e} = 0.083$ and the corresponding values of $\frac{M}{M_e} = 0.917$. Thus the load P = 0.083 x 67500 = 5600 lb.

The maximum elastic deflection Δ_e occurring at the threshold of inelastic strain in the beam is found by substituting P = 5600 into Eq. 12 with the result that $\Delta_e = 0.06$ in.

(b) Load for Inelastic Strain to One-Half Depth. For this solution we rewrite Eq. 2 to include the bending moment at the most stressed section, namely the mid-point due to the load W = -P. This equation is Eq. 9 in which $y = -\Delta_{max}$, $x = \frac{\ell}{2}$ and $M_1 = Pe_o$.

$$M = Pe_o - P\Delta + \frac{P\ell}{4} = P(e_o - \Delta + \frac{\ell}{4}) \qquad (16)$$

As in problem 1, we substitute for Δ in Eq. 16 a value of $2\Delta_e = 0.12$ in. Thus Eq. 16, with these quantities substituted, becomes

$$M = P(0.3 - 0.12 + 2.06) = 2.24P$$

By dividing both sides of the latter equation by M_e it becomes

$$\frac{M}{M_e} = 2.24\frac{P}{M_e} = 2.24\frac{P}{\frac{\sigma_e I}{c}} = 2.24 \times \frac{3}{c}\frac{P}{P_e} = 10.7\frac{P}{P_e}$$

In Fig. 12 this latter equation represents a radial line which intersects the interaction curve for 1/2 depth of inelastic strain at a point whose coordinates are $\frac{P}{P_e} = 0.125$ and $\frac{M}{M_e} = 1.37$. Therefore $P = 0.125P_e = 8700$ lb. A comparison of 8700 lb. with 5600 lb. shows a 55 percent increase in the load at the threshold of occurrence of inelastic strain is required to cause inelastic strains in the most stressed cross-section to occur to a depth of one-half the cross-section.

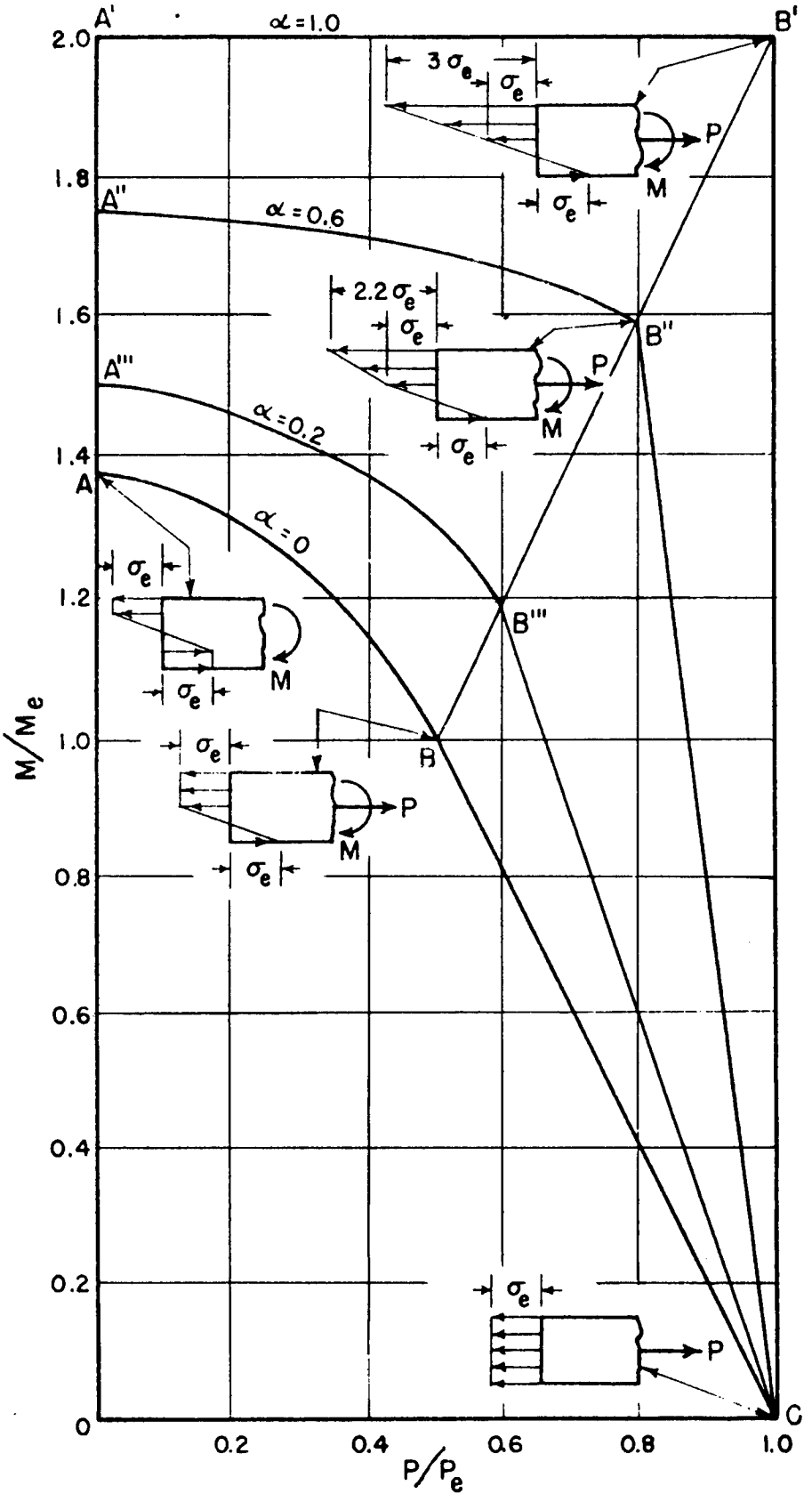

FIG. 1 THE EFFECT OF THE STRAIN HARDENING FACTOR α ON MOMENT-LOAD INTERACTION CURVES FOR A MEMBER OF RECTANGULAR CROSS-SECTION WITH HALF THE DEPTH YIELDED.

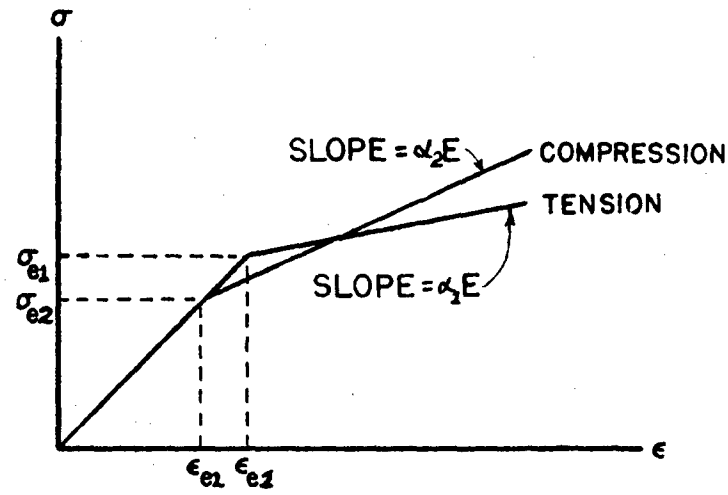

(a) IDEALIZED STRESS-STRAIN DIAGRAMS FOR MATERIAL

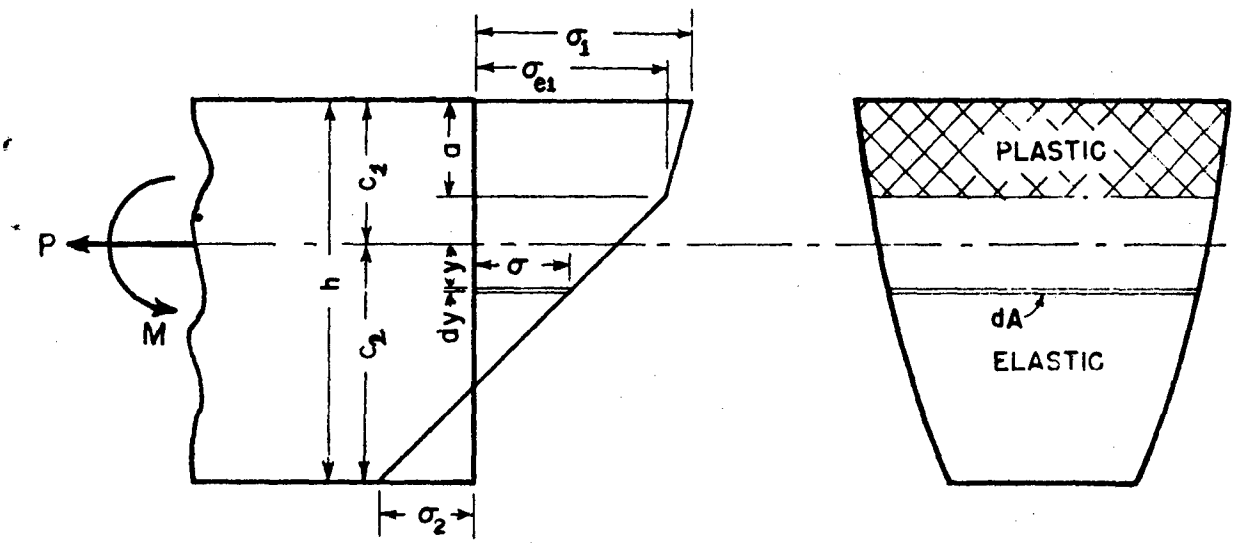

(b) STRESS-DISTRIBUTION

(c) CROSS-SECTION

FIG. 2 DISTRIBUTION OF STRESS IN A STRAIGHT MEMBER OF SYMMETRICAL CROSS-SECTION WHICH IS SUBJECTED TO AXIAL TENSION AND BENDING LOADS.

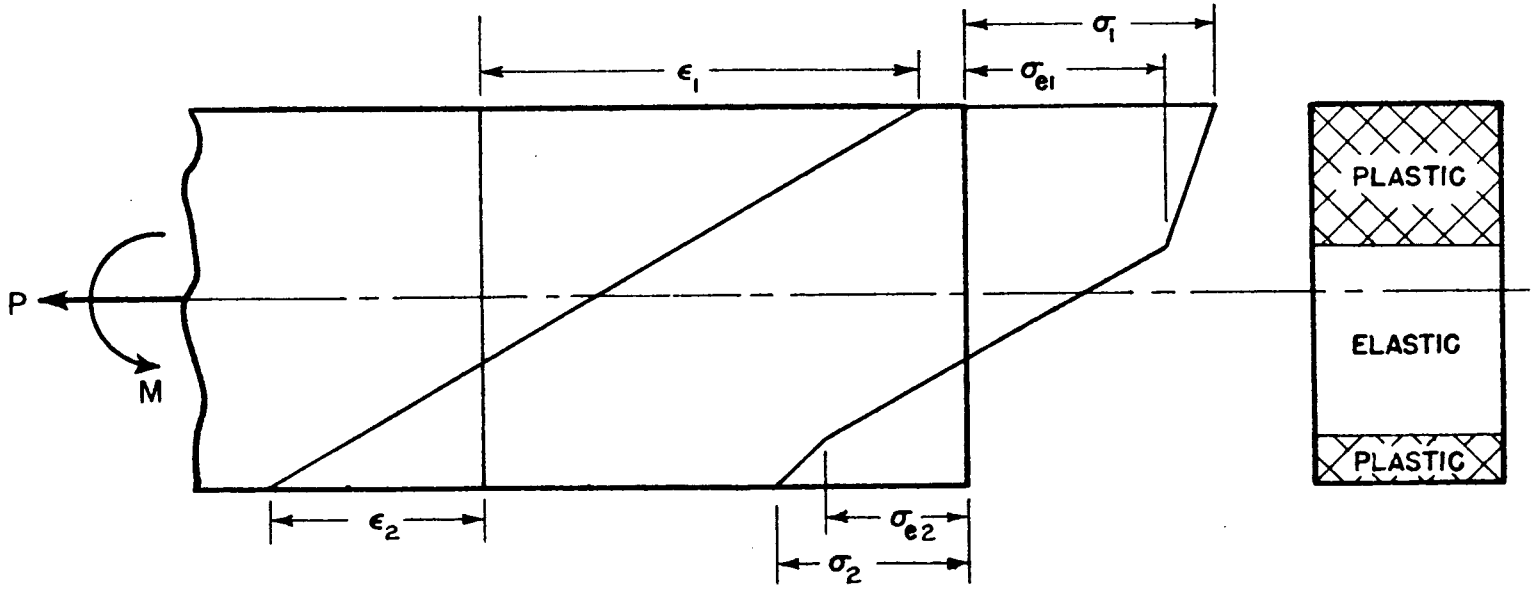

(a) STRAIN-DISTRIBUTION (b) STRESS-DISTRIBUTION (c) CROSS-SECTION

FIG. 3 DISTRIBUTION OF STRAIN AND STRESS IN A STRAIGHT MEMBER OF RECTANGULAR CROSS-SECTION WHICH IS SUBJECTED TO AXIAL TENSION AND BENDING LOADS.

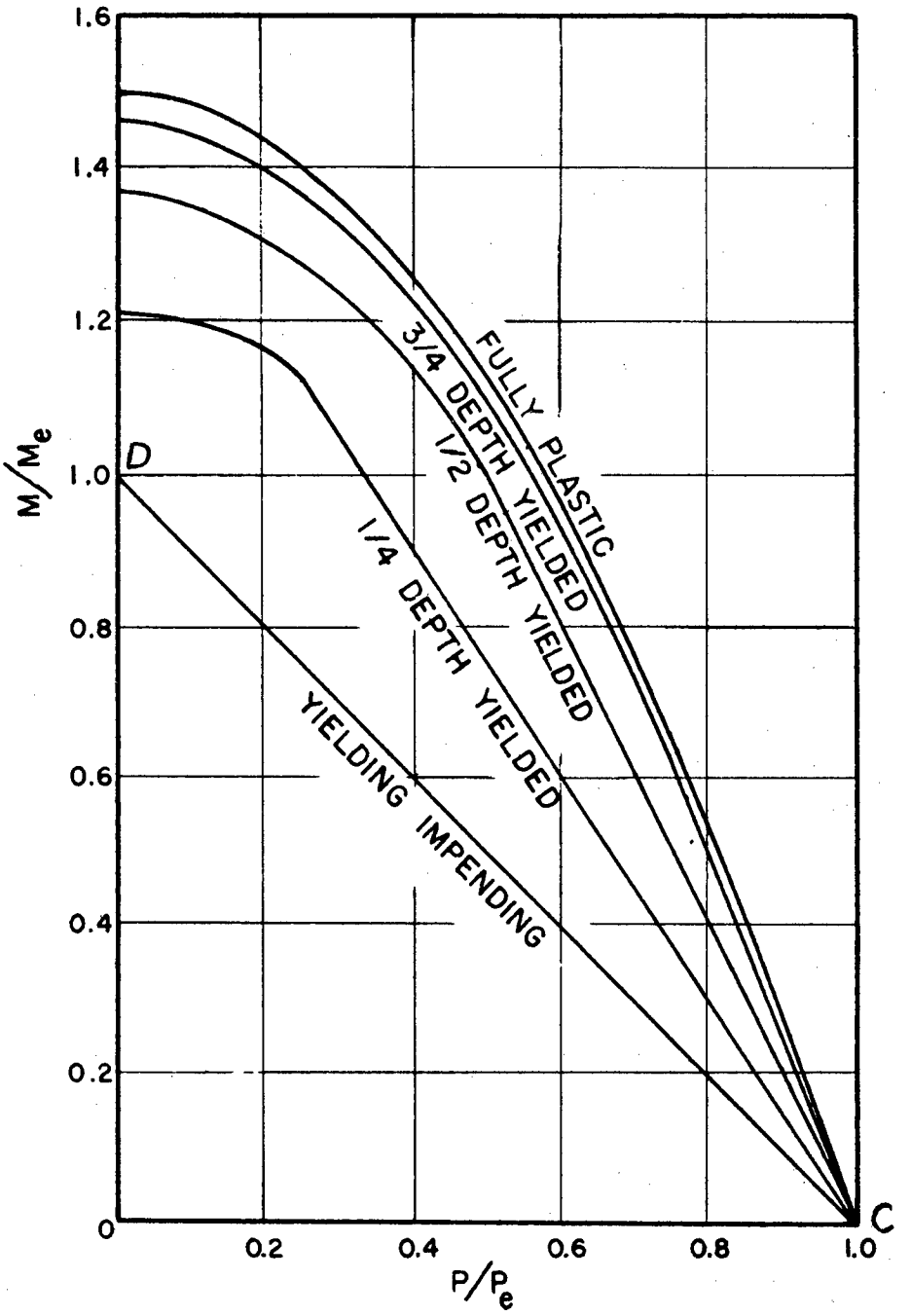

FIG. 4 THE EFFECT OF DEPTH OF YIELDING ON THE MOMENT-LOAD INTERACTION CURVES FOR A MEMBER OF RECTANGULAR CROSS-SECTION MADE OF A MATERIAL WITH $\alpha = 0$.

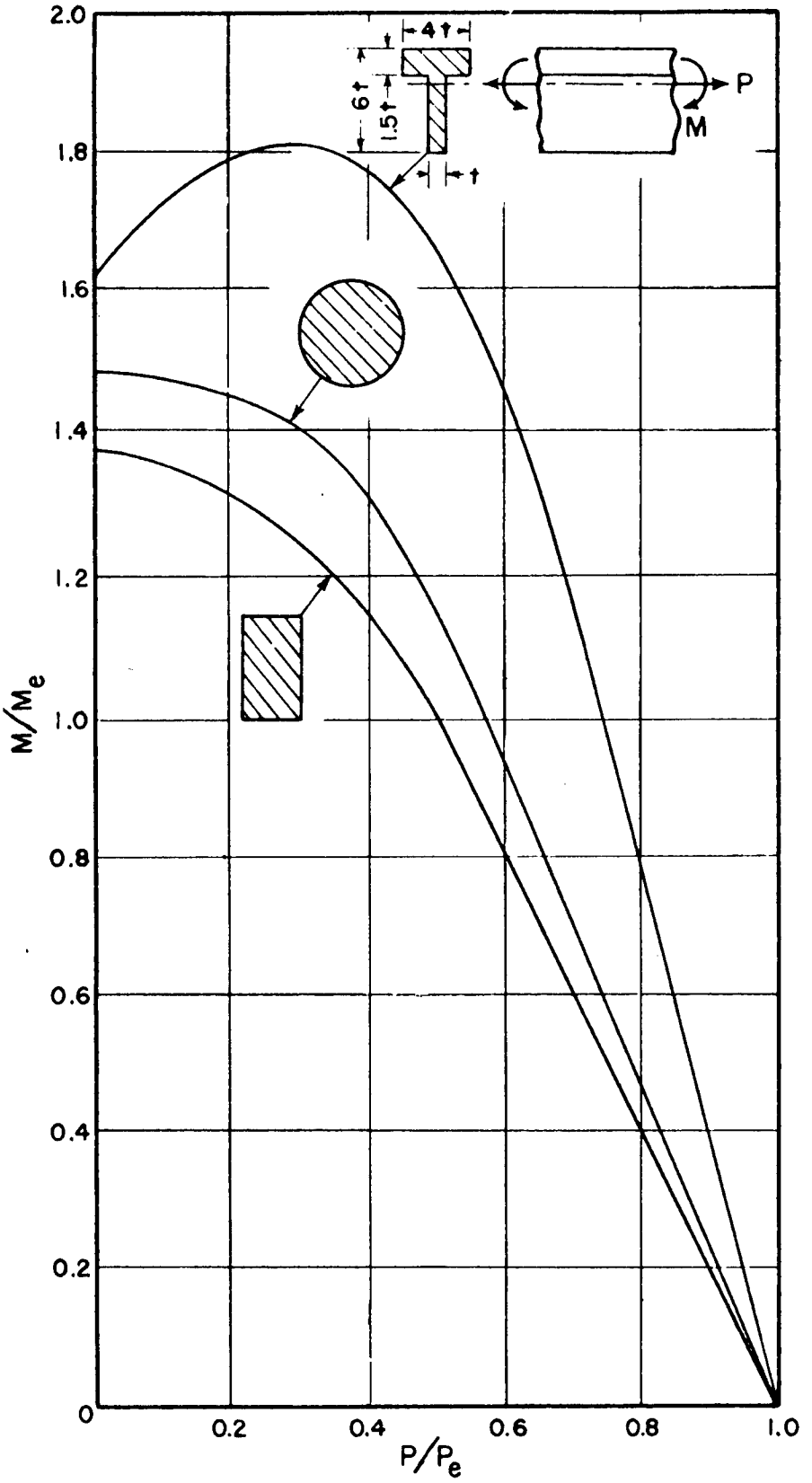

FIG. 5 THE EFFECT OF CROSS-SECTION ON THE MOMENT-LOAD INTERACTION CURVES FOR A MEMBER MADE OF A MATERIAL WITH $\alpha = 0$.

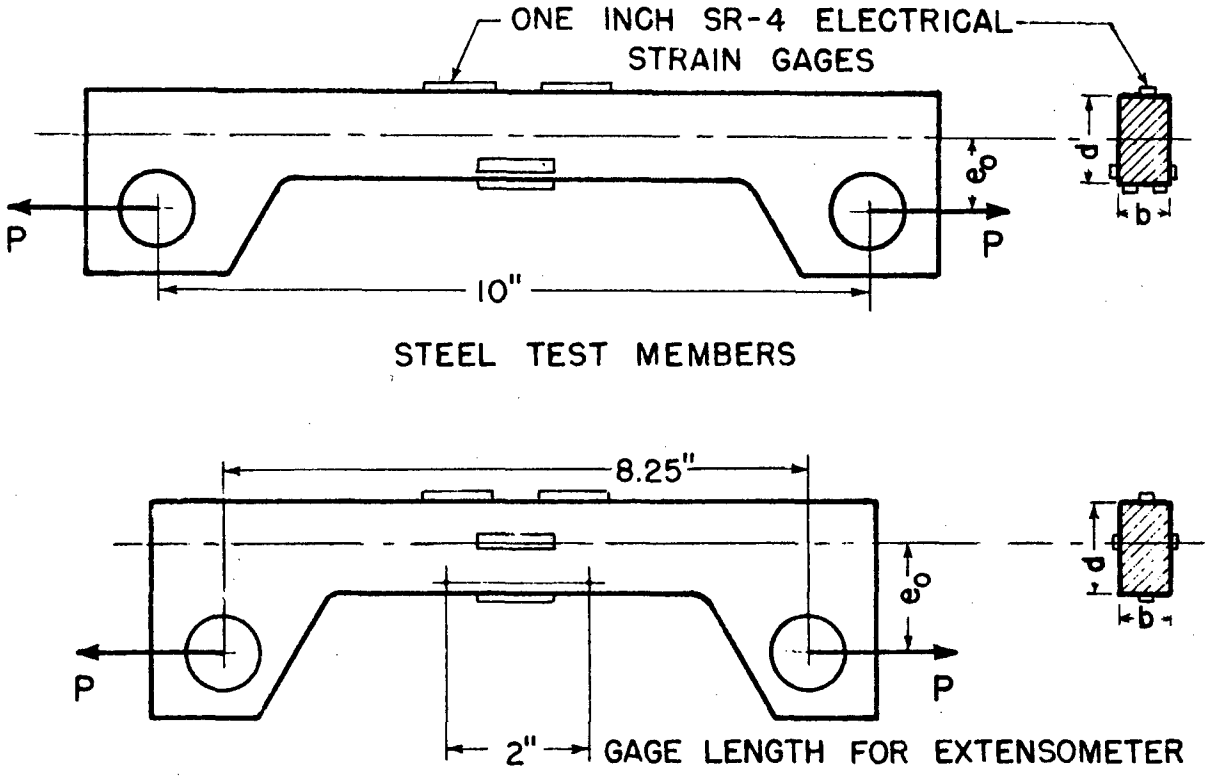

FIG. 6 SKETCHES OF TEST MEMBERS SHOWING MANNER OF LOADING.

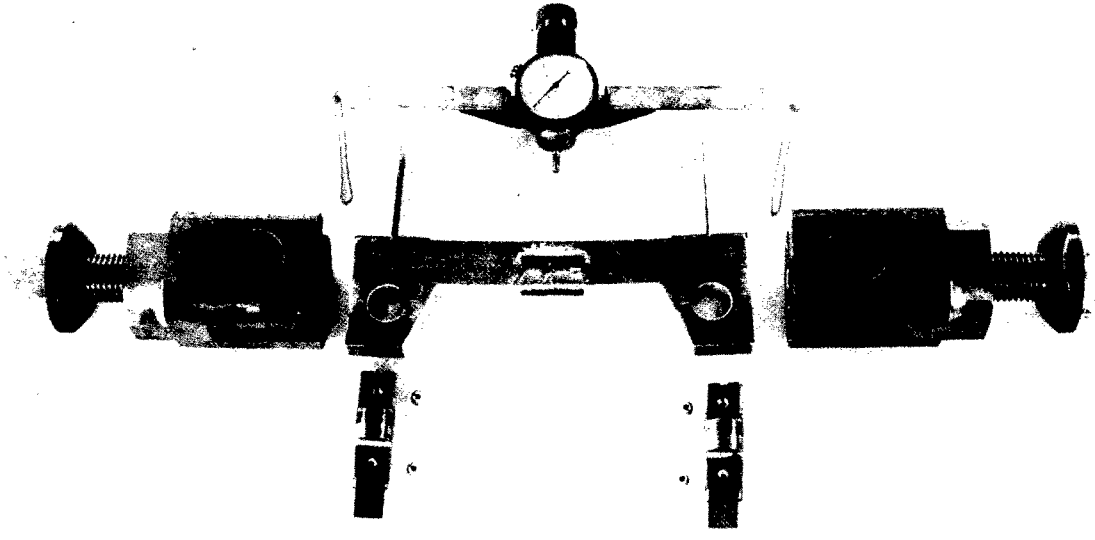

FIG. 7 LAYOUT OF FIXTURES USED IN LOADING TEST MEMBERS

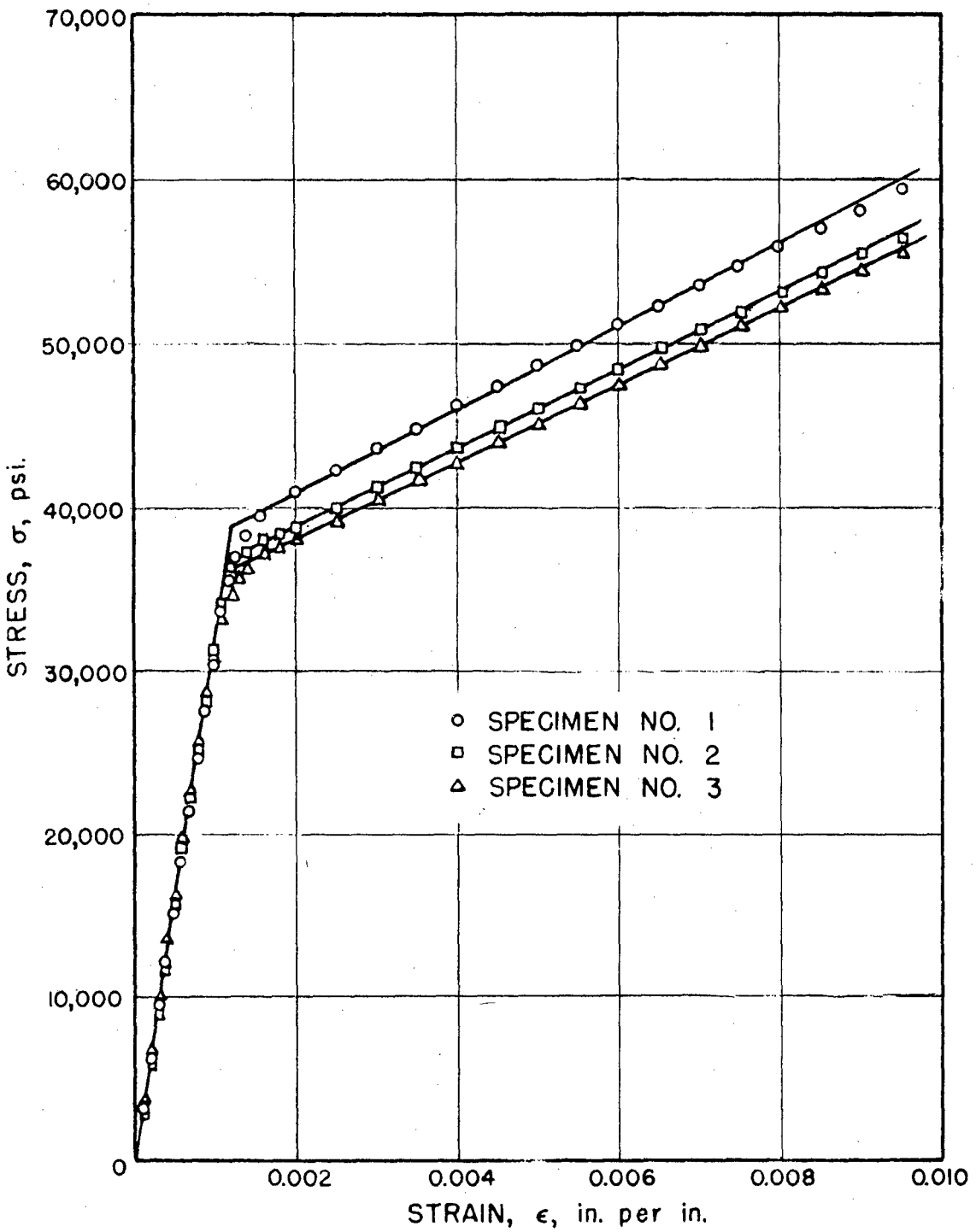

FIG. 8 TENSION STRESS-STRAIN DIAGRAMS OF ANNEALED RAIL STEEL.

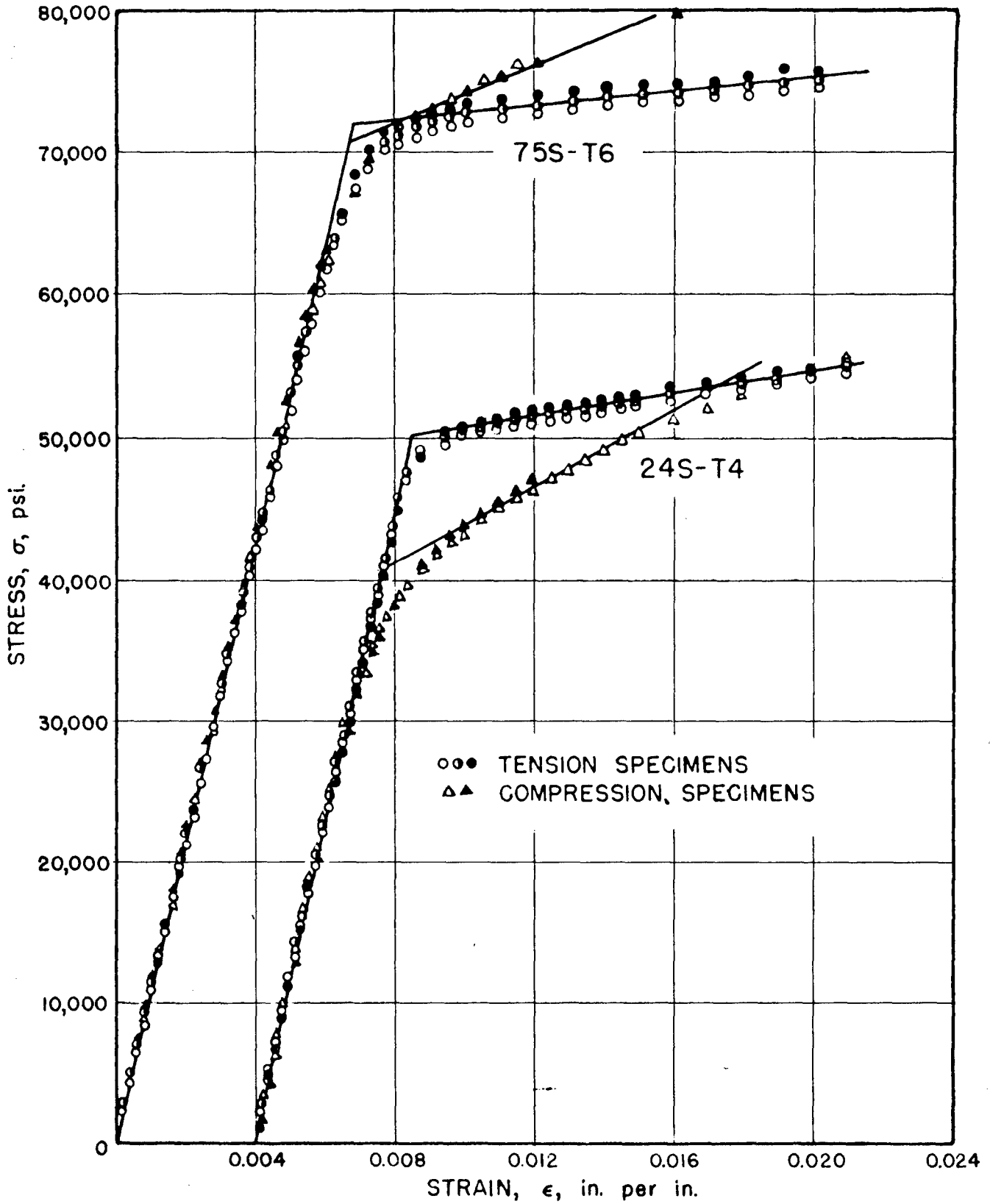

FIG. 9 COMPOSITE TENSION AND COMPRESSION STRESS-STRAIN DIAGRAMS OF ALUMINUM ALLOYS 24S-T4 AND 75S-T6.

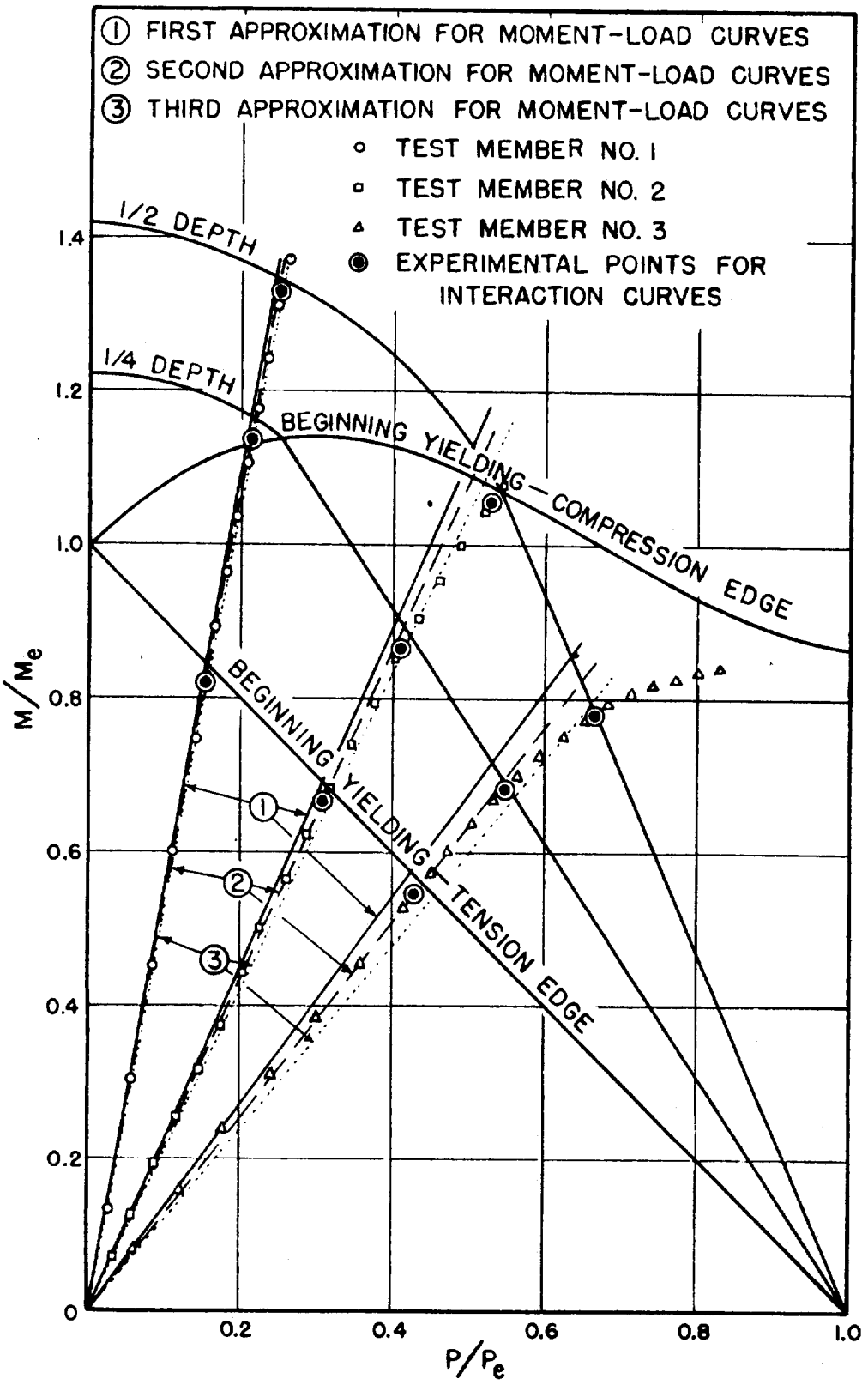

FIG. 10 COMPARISON OF EXPERIMENTAL AND THEORETICAL INTERACTION AND MOMENT-LOAD CURVES FOR RAIL STEEL TEST MEMBERS OF RECTANGULAR CROSS-SECTION.

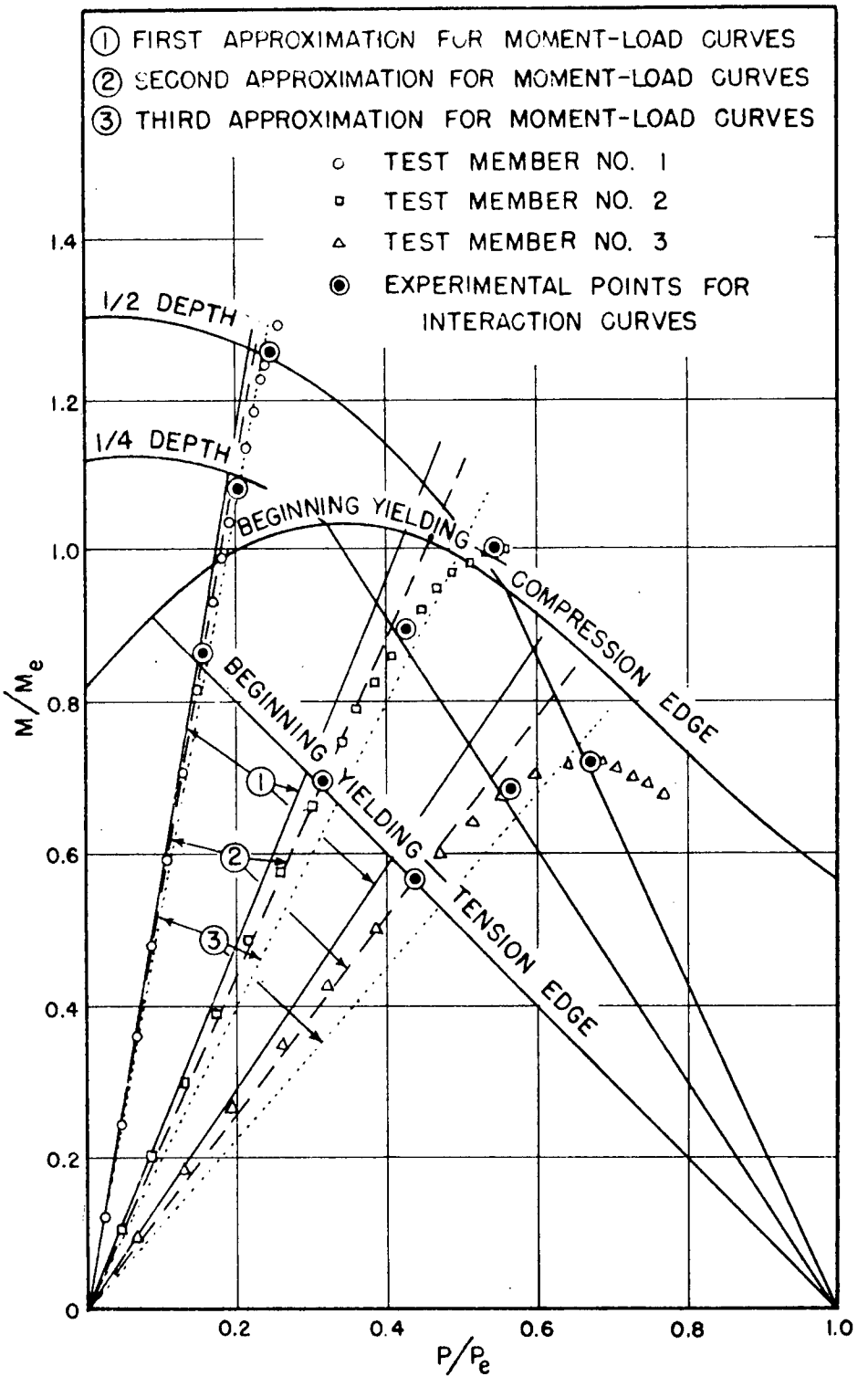

FIG. 11 COMPARISON OF EXPERIMENTAL AND THEORETICAL INTERACTION AND MOMENT-LOAD CURVES FOR ALUMINUM ALLOY 24S-T4 TEST MEMBERS OF RECTANGULAR CROSS-SECTION.

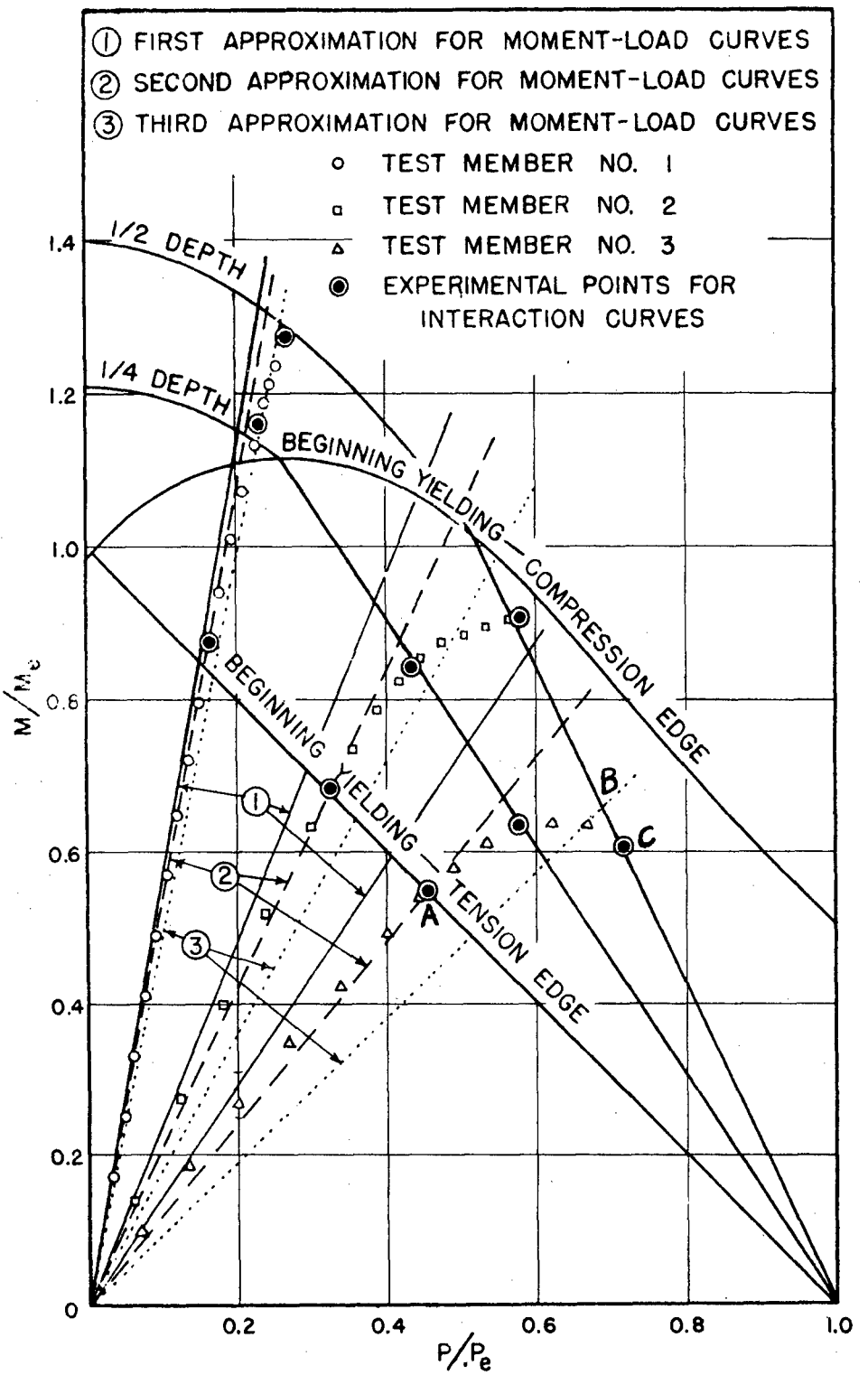

FIG. 12 COMPARISON OF EXPERIMENTAL AND THEORETICAL INTERACTION AND MOMENT-LOAD CURVES FOR ALUMINUM ALLOY 75S-T6 TEST MEMBERS OF RECTANGULAR CROSS-SECTION.

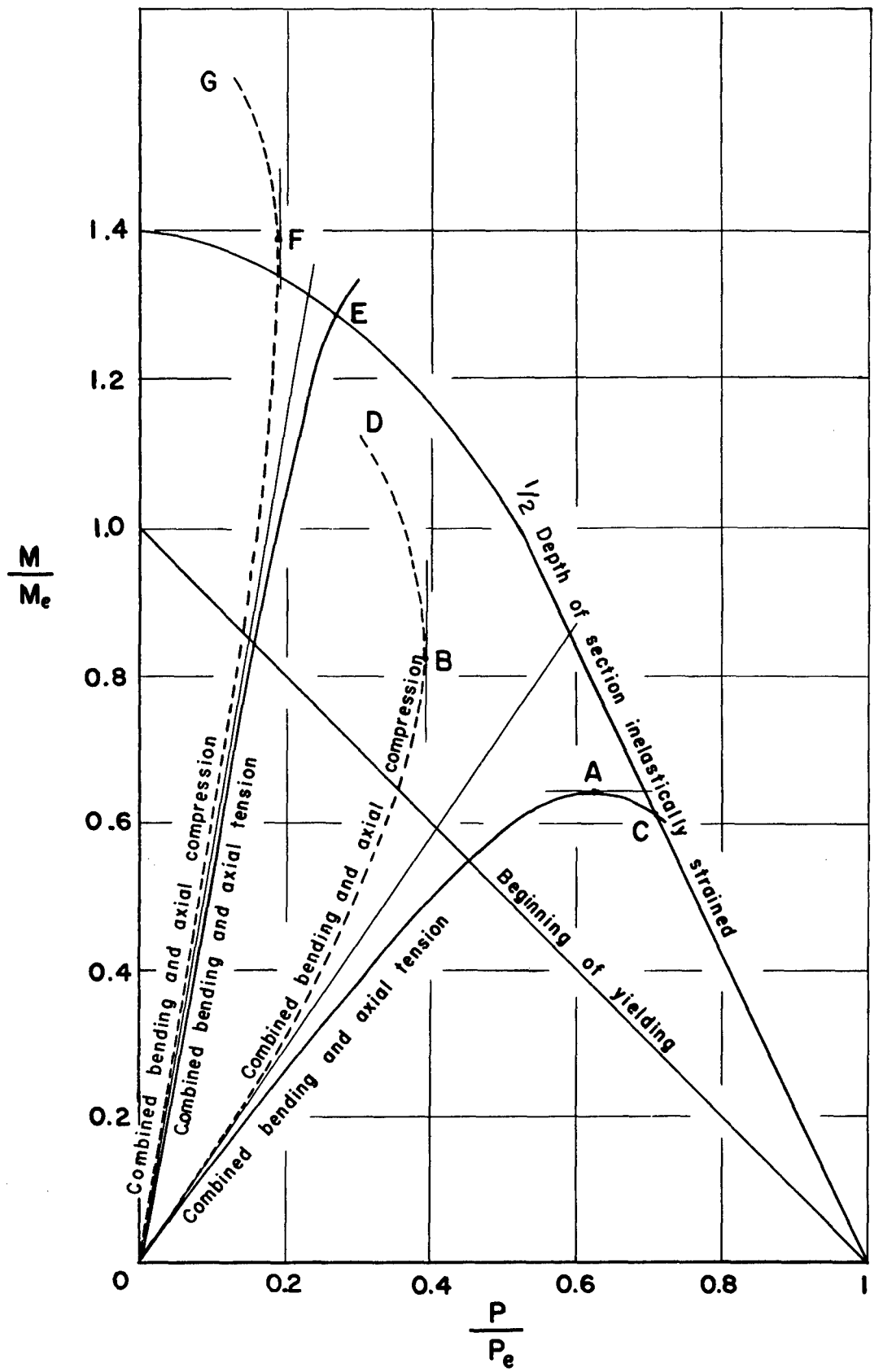

FIG 13 MOMENT-LOAD CURVES CONTRASTING THE EFFECT OF TENSILE AXIAL LOADS WITH COMP. AXIAL LOADS ON FAILURE OF MEMBER

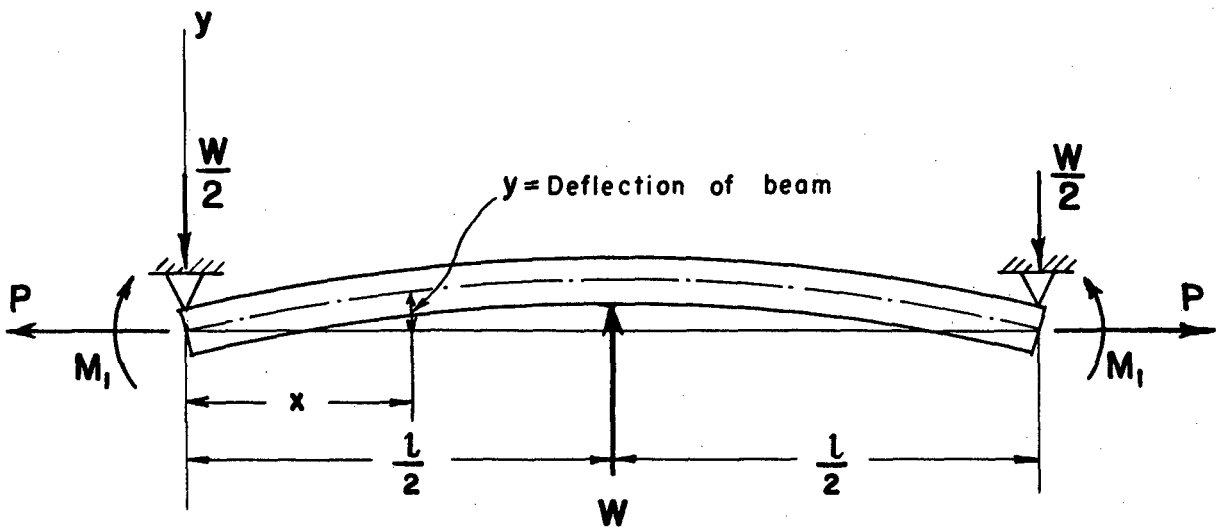

FIG 14 COMBINED AXIAL AND BENDING LOADING